Neurobiology of Stress 34 (2025) 100696

Contents lists available at ScienceDirect

Neurobiology of Stress

journal homepage: www.elsevier.com/locate/ynstr

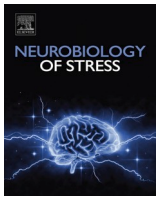

Elevated GABAergic neurotransmission prevents chronic intermittent ethanol induced hyperexcitability of intrinsic and extrinsic inputs to the ventral subiculum of female rats

Eva C. Bach *, Jeff L. Weiner

Department of Translational Neuroscience, Wake Forest University, School of Medicine, Medical Center Boulevard, Winston-Salem, NC 27157, USA

A B S T R A C T

With the recent rise in the rate of alcohol use disorder (AUD) in women, the historical gap between men and women living with this condition is narrowing. While there are many commonalities in how men and women are impacted by AUD, an accumulating body of evidence is revealing sex-dependent adaptations that may require distinct therapeutic approaches. Preclinical rodent studies are beginning to shed light on sex differences in the effects of chronic alcohol exposure on synaptic activity in a number of brain regions. Prior studies from our laboratory revealed that, while withdrawal from chronic intermittent ethanol (CIE), a commonly used model of AUD, increased excitability in the ventral hippocampus (vHC) of male rats, this same treatment had the opposite effect in females. A follow-up study not only expanded on the synaptic mechanisms of these findings in male rats, but also established a CIE-dependent increase in the excitatory-inhibitory (E-I) balance of a glutamatergic projection from the basolateral amygdala to vHC (BLA-vHC). This pathway modulates anxiety-like behavior and could help explain the comorbid occurrence of anxiety disorders in individuals suffering from AUD. The present study sought to conduct a similar analysis of CIE effects on both synaptic mechanisms in the vHC and adaptations in the BLA-vHC pathway of female rats. Our findings indicate that CIE increases the strength of inhibitory neurotransmission in the vHC and that this sex-specific adaptation blocks, or at least delays, the increases in intrinsic vHC excitability and BLA-vHC synaptic transmission observed in males. Our findings establish the BLA-vHC pathway and the vHC as important circuitry to consider for future studies directed at identifying sex-dependent therapeutic approaches to AUD.

1. Introduction

Although alcohol use disorder (AUD) has historically been thought of as a disease that predominantly impacts men, sex differences in both the rates of binge drinking and the prevalence of AUD have been steadily declining as women's engagement in these behaviors has increased (Giacometti and Barker, 2020; Grant et al., 2017; Guinle and Sinha, 2020; Han et al., 2017; White et al., 2015). The reasons for the sex-dependent divergence in AUD trends have remained largely conjecture due, at least in part, to a historical dearth of clinical and preclinical studies conducted in women or female experimental subjects. As this serious omission is now finally being corrected, both basic and clinical studies are discovering robust sex differences in some of the neurobiological and associated behavioral adaptations that develop following chronic alcohol exposure. These sexually dimorphic effects may argue for a need to consider sex-specific therapeutic approaches to combat AUD (Flores-Bonilla and Richardson, 2020).

Despite the differences noted above, both men and women suffering from AUD are often diagnosed with comorbid anxiety-, depressive and post-traumatic stress disorders. These conditions can both precipitate and exacerbate AUD (Gilpin and Weiner, 2017; Guinle and Sinha, 2020). Moreover, dysregulation of stress circuitry plays an integral role in prominent theories of AUD (Koob and Volkow, 2016). Rodents undergoing withdrawal from chronic intermittent ethanol vapor exposure (CIE), a commonly used model of AUD, show anxiety- and depressive-like behaviors during withdrawal from CIE. Given the close link between AUD, stress, and these other mental health disorders it has come as no surprise that many of the brain regions and associated pathological adaptations driving these conditions are shared. The basolateral amygdala (BLA) and the ventral hippocampus (vHC) are two

Abbreviations: CIE, Chronic intermittent ethanol exposure; AUD, Alcohol use disorder; BLA, Basolateral Amygdala; vSub, Ventral subiculum; vHC, Ventral hippocampus; E-I, Excitatory to inhibitory; ChR2, Channelrhodopsin; BEC, Blood ethanol concentrations; oEPSC, Optically evoked excitatory postsynaptic currents; oIPSC, Optically evoked inhibitory postsynaptic currents; moEPSC, Monosynaptic optically evoked excitatory postsynaptic currents; moIPSC, Monosynaptic optically evoked inhibitory postsynaptic currents; sEPSC, spontaneous excitatory postsynaptic currents; sIPSC, spontaneous inhibitory postsynaptic currents; PPr, Paired-pulse ratios; ISI, Interstimulus interval; TTX, Tetrodotoxin; PTX, Picrotoxin.

* Corresponding author. PTCRC, 115 S. Chestnut Street, Winston-Salem, NC 27101, USA.
E-mail address: ebach@wakehealth.edu (E.C. Bach).

https://doi.org/10.1016/j.ynstr.2024.100696

Available online 21 November 2024

such interconnected brain regions (Almonte et al., 2017; Blaine and Sinha, 2017; Chappell et al., 2013; Grace et al., 2021; Rau et al., 2015; Silberman et al., 2009). Studies in male rats have consistently shown evidence for hyperexcitablity of BLA pyramidal neurons in response to ethanol dependence and a variety of chronic stress models (Blume et al., 2019; Christian et al., 2012; Lack et al., 2007; Rau et al., 2015). The picture of alcohol dependence- and/or anxiety-driven BLA adaptations in female rats has proven more complex. Studies with female rats undergoing withdrawal from CIE initially suggested that they develop hyperexcitability in principal neurons of the BLA similar to their male counterparts but that they simply require more prolonged exposure to CIE (Morales et al., 2018). Follow-up studies refined the hypothesis that only a subset of BLA projections neurons experience hyperexcitability driven by CIE while others remained unaffected (Price and McCool, 2022). In line with sex-dependent BLA adaptations, evidence in the clinical population has revealed a reduction in BLA volumes in abstinent alcohol dependent men but not women (Grace et al., 2021). Moreover, at least one group has reported that a rodent model of chronic stress actually leads to a reduction in BLA pyramidal cell excitability in females, possibly as a consequence of sex- and estrous cycle-dependent differences in baseline activity measures (Blume et al., 2017, 2019).

The BLA is thought to regulate anxiety via monosynaptic projections to a variety of cortical and subcortical structures (Felix-Ortiz et al., 2013; Felix-Ortiz et al., 2016; Kim et al., 2013; Pi et al., 2020; Vantrease et al., 2022). An excitatory projection from the BLA to vHC can modulate anxiety-like behaviors and alcohol seeking (Bach et al., 2023; Felix-Ortiz et al., 2013; Pi et al., 2020). Moreover, models of acute and chronic stress promote intrinsic vHC hyperexcitability and lesions to the vHC elicit behavioral phenotypes consistent with eliciting an anxiolytic phenotype. Importantly, to date all studies looking at the role of the BLA-vHC pathway and the vHC on anxiety-like behaviors in rodents have been limited to male subjects. Although the specific vHC subregions involved in these behavioral effects are not always elucidated, in agreement with anatomical studies of projection targets, both the vCA1 and the ventral subiculum (vSub) appear to represent primary players in mediating anxiety-like behaviors (Almonte et al., 2017; Bannerman et al., 2004; Chang and Gean, 2019; Chang et al., 2015; Felix-Ortiz et al., 2013; Kondev et al., 2023).

The frequent comorbidity between AUD and anxiety disorders prompted our prior studies looking at synaptic plasticity induced by CIE in the vHC of male and female rats. These studies revealed that both sexes exhibited anxiety-like behaviors during acute withdrawal from CIE, although these phenotypes were less pronounced in females. Moreover, this same treatment led to increased extracellular neural excitability in the vHC CA1 region in males while reducing this measure in females (Bach et al., 2021b; Ewin et al., 2019). In a follow up study, looking at individual neurons within the vSub, we confirmed an increase in intrinsic excitatory neurotransmission of this region in male rats. We also showed that CIE increased synaptic excitability in the BLA-vSub pathway (Bach et al., 2021a).

In the present study we extended our investigation to explore CIE-dependent neuronal adaptations in vSub excitability and the BLA-vSub pathway in female rats. Using optogenetic approaches we found CIE to have no effect on monosynaptically evoked BLA inputs to the vSub, although polysynaptic driven inputs, engaging intrinsic activity of the vSub, did become strengthened. Importantly, while the excitatory-inhibitory (E-I) balance of the overall BLA-driven input was disrupted (excitation increased) in male rats, it remained unaltered in females. The intrinsic vSub adaptations we previously observed in male rats are likely an important player in these sex-dependent adaptations. In males, CIE increased intrinsic excitatory neurotransmission while inhibition remained unaffected (Bach et al., 2021a). In female rats we found opposite intrinsic vSub adaptations, with CIE leading to an increase in inhibitory drive and no effect on excitation. Importantly, we also found that blocking this elevated inhibitory drive unmasked BLA-vSub and intrinsic vSub hyperexcitability in female rats. Taken together our findings support sex-dependent adaptations in response to CIE, particularly in the GABA system, that at least initially decrease susceptibility to hyperexcitation in BLA-vSub pathway-driven and intrinsic vSub inputs of female rats.

2. Methods

Female Long Evans rats were purchased from Inotiv, IN and arrived between 9 and 10 weeks. Upon arrival rats were singly housed in clear cages (25.4 cm × 45.7 cm) and maintained on a 12:12 h light dark cycle. Rats had ad libitum access to food (Prolab RMH 3000, LabDiet: PMI Nutrition International, St. Louis, MO) and water throughout the study. Animal care procedures were carried out in accordance with the NIH Guide for the Care and Use of Laboratory Animals and were approved by the Wake Forest University Animal Care and Use Committee. All animal care and use procedures were carried out in compliance with ARRIVE guidelines. A total of 15 CIE and 16 AIR rats were used to complete all electrophysiological studies. A total of 126 (65 Air and 61 CIE) cells were recorded from to complete electrophysiological studies.

2.1. Stereotactic surgeries

Naïve subjects weighing between 200 and 230 g were anesthetized using sodium pentobarbital (40–50 mg/kg, i.p.). For analgesic purposes animals were injected subcutaneously with 2 mg/kg meloxicam. The scalp was shaved and surgically scrubbed. Rats were placed in a stereotaxic frame and an incision was made centrally along the scalp. A craniotomy positioned directly above the posterior BLA (stereotaxic coordinates in mm were AP: 3.1 ML: 4.5 and DV:7.8) was made bilaterally to allow microinjection needles to be lowered into the posterior BLA (BLA). Microinjection needles were used to transfect the BLA with 0.8–0.9 μL of a virus construct (pAAV5-CaMKIIa-hChR2(H134R)-EYFP) expressing the excitatory opsin, channelrhodopsin (ChR2) at a rate of 2 μL/min (Addgene, Cambridge, MA). Microinjection needles were maintained in place for 5 min before being withdrawn. Animals were sutured and allowed to recover in their home cages. The viral construct was allowed to express and traffic to BLA terminals for the following 5–6 weeks (the variability in expression window was due to our need to stagger the animals to conduct electrophysiological recordings) and subsequently exposed to 10 days of chronic intermittent ethanol vapor inhalation or air exposure.

2.2. Chronic intermittent ethanol vapor inhalation exposure

All animals (Air control and CIE) were housed in their standard home cages on a reverse light cycle (9 p.m.–9 a.m.). Home cage housed animals in the CIE condition were placed in custom-built Plexiglas chambers (Triad Plastics, Winston-Salem, NC) to allow ethanol vapor to be pumped into the chamber for 12 h a day over the course of 10 days. Animals were weighed daily and tail blood samples were taken a minimum of 3 times during the 10 day CIE paradigm. Ethanol concentrations were adjusted maintain the animal's blood ethanol concentrations (BECs) at 150–225 mg/dl. Following the 10 day procedure, ethanol exposed rats underwent 24 h of withdrawal (no ethanol vapor) before being sacrificed for electrophysiological recordings. Animals in the Air condition were similarly housed in their home cages and exposed only to room air. Throughout the 11 day duration leading up to the electrophysiological recordings Air animals were and handled daily (placed in weigh boat and handling cloth while the tail was manipulated) to mimic handling of ethanol exposed animals. All animals (Air and CIE) were sacrificed for electrophysiological recordings at 9 a.m. ± 1 h.

2.3. Blood ethanol concentrations

Blood ethanol concentrations (BECs) were determined from a 10 μL sample of tail vein blood obtained via tail snip from each individual rat.

BECs were determined using a commercially available alcohol dehydrogenase enzymatic assay kit (Carolina Liquid Chemistries Corporation, Brea, CA). Ethanol concentrations were then determined using a spectrophotometer (Molecular Devices Spectra Max). The average BEC of all included animals was 177.13 ± 7.9 mg/dL.

2.4. Electrophysiology

Electrophysiological experiments were conducted following 24 h of withdrawal from CIE. Animals were deeply anesthetized using isoflurane. Following decapitation, the brain was removed rapidly and suspended in ice-cold NMDG recovery solution containing in mM: 92 NMDG, 2.5 KCl, 1.25 NaH_2PO_4, 30 $NaHCO_3$, 20 HEPES, 25 glucose, 2 thiourea, 5 Na-ascorbate, 3 Na-pyruvate, 0.5 $CaCl_2{\cdot}2H_2O$, and 10 $MgSO_4{\cdot}7H_2O$. NMDG was titrated to pH 7.4 with 17 mL ± 0.5 mL of 5 M hydrochloric acid (REFS). Transverse slices containing the vHC were cut at a thickness of 300 μm using a VT1000S Vibratome (Leica Microsystems). vHC slices were placed in a holding chamber containing NMDG recovery solution. Slices were allowed to recover for 35 min before being transferred to a chamber filled with artificial cerebral spinal fluid (aCSF) containing in mM: 125 NaCl, 1.25 NaH_2PO_4, 25 $NaHCO_3$, 10 D-Glucose, 2.5 KCl, 1 $MgCl_2$, and 2 $CaCl_2$. NMDG recovery and aCSF holding solutions were oxygenated with 95% O_2 and 5% and warmed to 32–34 °C. For recordings, a single brain slice was transferred to a chamber mounted on a fixed stage under an upright microscope (Scientifica SliceScope Pro, 2000 microscope), where it was superfused continuously with warmed oxygenated aCSF. Whole-cell voltage-clamp recordings were made in presumptive pyramidal neurons of the ventral subiculum (vSub) using recording pipettes pulled from borosilicate glass (open tip resistance of 6–9 MΩ; King Precision Glass Co., Claremont, CA). The pipette solution contained (in mM): 130–140 Cs-gluconate, 10 HEPES, 1 NaCl, 1 $CaCl_2$, 3 CsOH, 5 EGTA, 2 Mg^{2+}-ATP, 0.3 GTP-Na_2 and 2 Qx-314. Intracellular Cs^+ was used as the primary cation carrier in voltage-clamp recordings to block K^+ currents, including postsynaptic $GABA_B$ receptor-mediated currents, in the recorded neuron. Neurons in the ventral subiculum (vSub) were targeted for recording under a 40 × water-immersion objective (numerical aperture = 0.8) with infrared-differential interference contrast (IR-DIC) optics, as described previously. Electrophysiological signals were obtained using a Multiclamp 700B amplifier (Molecular Devices, Union City, CA), low-pass filtered at 3 kHz, digitized at 10 kHz, and recorded onto a computer (Digidata 1440A, Molecular Devices) using pClamp 11.0 software (Molecular Devices). Series resistance, measured from brief voltage steps applied through the recording pipette (5 mV, 5 ms), was <25 MΩ and was monitored periodically during the recording. Recordings were discarded if series resistance changed by > 20% over the course of the experiment. Each recorded neuron represents an individual data point (n); recordings were made from at least four rats for each experimental group. To selectively stimulate terminals originating from the BLA and synapsing onto vSub neurons, blue light (473 nm) was delivered though the objective using an CoolLED driver (pE-300^{ulta}). For recordings of optically-evoked excitatory and inhibitory postsynaptic currents (oEPSCs and oIPSCs, respectively) and spontaneous excitatory and inhibitory postsynaptic currents (sEPSCs and sIPSCs, respectively) cells were voltage clamped at − 70 mV (near the theoretical IPSC reversal potential) and at 0 mV (near the theoretical EPSC reversal potential), respectively. To establish maximal monosynaptic amplitudes and polysynaptic areas under the curve cells, were stimulated for 5 ms and at 34 mW/mm^2 intensity with the cell centered over the light source. Optical stimulation was performed at 0.1 Hz to obtain at least 10 consecutive optically-evoked postsynaptic currents. To establish the excitatory and inhibitory ratio (E/I ratio), the total excitatory area under the curve was divided by the total inhibitory area under the curve when both could be obtained from the same neuron and a minimum recording duration of 2 min To assess the E/I ratio of spontaneous postsynaptic currents (sPSCs) the frequency, amplitude or synaptic drive (frequency x amplitude) of sEPSCs was divided by the same measure of sIPSCs (Levine et al., 2021). A minimum of 10 amplitude samples were averaged to arrive at an average response amplitude of presumptive monosynaptic oEPSCs. oEPSCs. Paired-pulse ratios (PPrs) were determined by delivering paired optical stimulations at an interstimulus interval (ISI) of 50,100 and 250 ms. Stimulation duration and intensity for PPr recordings were adjusted to obtain monosynaptic responses. PPrs were obtained by taking the ratio of the second and first amplitude (Amp2/Amp1). For recordings isolating α-amino-3-hydroxy-5-methyl-4-isoxazolepropionic acid (AMPA) receptor mediated oEPSCs cells and to establish the amplitude of NMDA-receptor- mediated oEPSCs cells were voltage-clamped at −80 and + 40 mV, respectively. To determine the AMPA/NMDA ratio, stimulation duration and intensities were adjusted to obtain a minimum of 10 oEPSCs. The maximum NMDA-mediated amplitude was determined by subtracting the area of AMPA mediated activity from the area of AMPA/NMDA-mixed component. The AMPA/NMDA ratio was calculated as the ratio between these isolated components.

2.5. Drug application

For a subset of experiments several pharmacological reagents were bath applied. Picrotoxin was bath applied to block $GABA_A$ receptors to pharmacologically isolate oEPSCs for AMPA receptor-mediated oEPSCs and AMPA/NMDA ratios. Recordings in the presence of Tetrodotoxin (TTX; 1–2 μM; Tocris Bioscience, Minneapolis, MN) were made to record action potential-independent optically evoked activity. 4-Aminopyradine (500 μM) was added in combination with TTX to unmask optically evoked activity blocked by TTX. Picrotoxin (100 μM; Sigma-Aldrich, St. Louis, MO) was added to the ACSF to block $GABA_A$ receptors. For specific experiments, DL-2-Amino-5-phosphonopentanoic acid (AP-5; 100 μM), NMDA (300 μM), and 6,7-dinitroquinoxaline-2,3-dione (DNQX; 20 μM; all from Sigma-Aldrich) was added to ACSF to block AMPA receptor mediated conductance.

2.6. Statistical analysis

Statistical analysis was performed using MiniAnlaysis, Matlab and Prism. The normality of measures (amplitudes, frequencies, areas, PPrs and ratios) was assessed using a Shapiro–Wilk test. Normally distributed data was analyzed using a two-tailed Student's T-Test, while non-normally distributed populations were compared using a Mann-Whitney Test to assess significant differences between the means of Air and CIE measures. Outliers were removed from all measures with the exception of sEPSC E/I ratios. Our rationale of this exception was that cells considered outliers were not consistent across the different E/I ratio measures (frequency, amplitude and synaptic drive) or for cells with primary measures (frequency or amplitude). Conducting a secondary analysis of E/I ratios following the removal of outliers did not qualitatively alter any of our reported conclusion (all E/I ratio measures of sEPScs were not different between groups). A repeated measures ANOVA with a post hoc Bonferroni's multiple comparison test was used to test the effect of multiple ISIs of oEPSC. PPRs for cells in which all ISIs were assessed in a single neuron. A repeated measures mixed-effects model with a post hoc Bonferroni's multiple comparison test was used to compare effects of CIE treatment on all cells. All results were considered statistically significant with a $p < 0.05$. Errors are reported as ± SEM.

3. Results

One of the primary objectives of this study was to explore the role of CIE on synaptic transmission driven by BLA inputs to the vSub in female rats. To address this question, we virally transfected the BLA with a virus expressing the excitatory opsin, channelrhodopsin (ChR2). Subsequent to a trafficking window of 6 weeks, we targeted pyramidal neurons in the vSub for electrophysiological recordings while optically stimulating

BLA fibers synapsing onto the recorded neuron using blue light (473 nm). We first measured optically evoked excitatory postsynaptic currents (oEPSCs) at −70 mV (near the IPSC reversal potential) (Smith et al., 2000). Inputs from the BLA elicited short latency oEPSCs (<5 ms) indicative of monosynaptic BLA inputs.

To assess the effect of CIE we first compared the amplitude of isolated (addition of TTX and 4AP) monosynaptic oEPSCs (moEPSCs) of Air and CIE rats. We did not identify a change in monosynaptic BLA moEPSC amplitude ($p = 0.5556$, Air cell n = 9, rat n = 5; CIE n = 13, rat n = 7; Mann-Whitney Test; Fig. 1B and C) or moEPSC area ($p = 0.7938$, Air n = 9, CIE n = 13; Mann-Whitney Test; data not illustrated graphically). Based on the latency of oPSCs (Fig. 1G) we identified a majority oEPSCs (88%) to have a monosynaptic component while the remaining cells (12%) showed only a polysynaptic component. In cells with a monosynaptic component the complexity (multiple recurrent peaks and duration of the response) suggested that the majority of oPSCs received recurrent network excitation thus consisting of both mono-as well as polysynaptic input. While the majority of oIPSC input was purely polysynaptic (56%) a subpopulation of vSub neurons received both mono- and polysynaptic BLA input (44%) (Fig. 1G). Given the complex

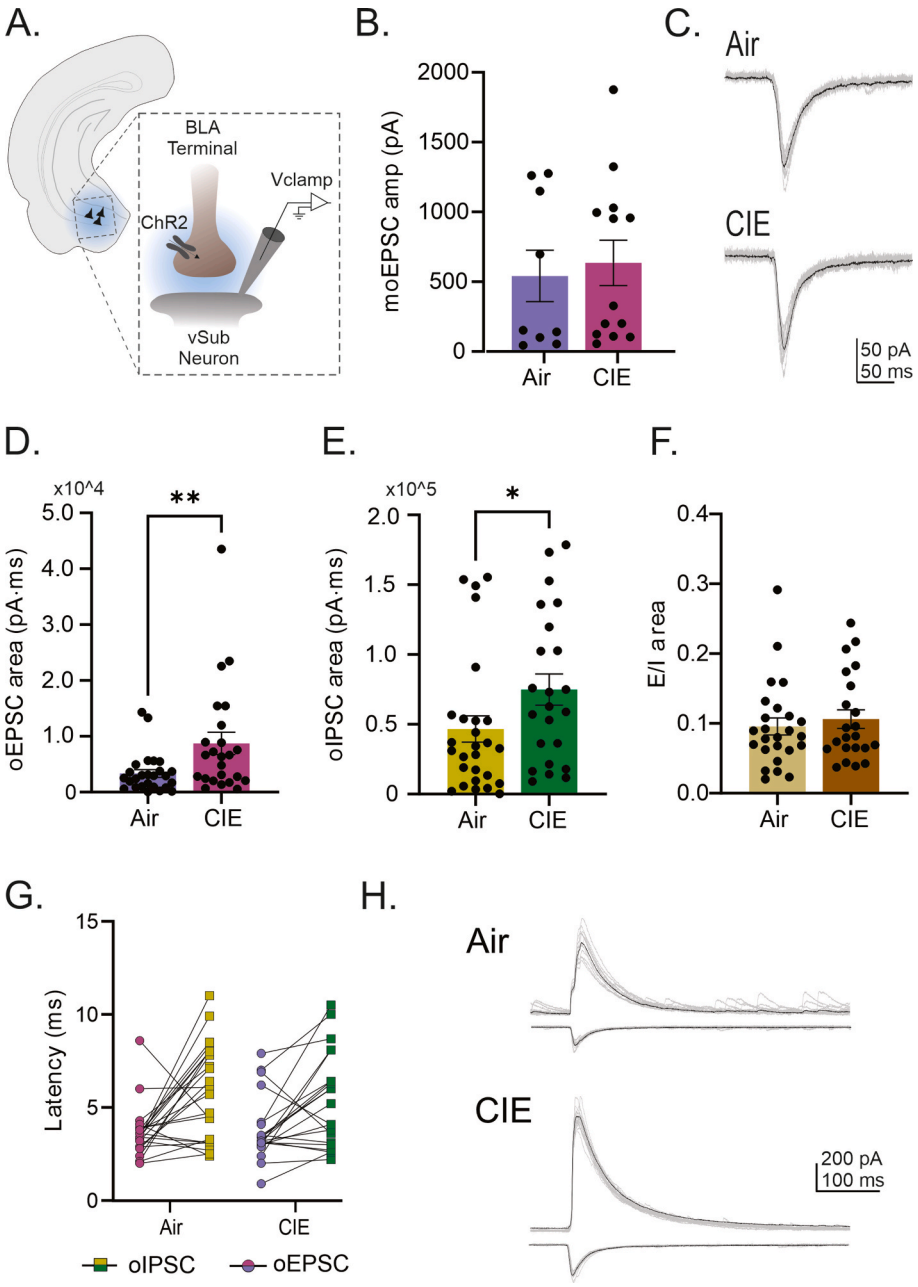

Fig. 1. Poly-, but not monosynaptic, excitatory BLA inputs to the vSub are strengthened in response to CIE without impacting the E-I balance. A) Schematic illustration of recording configuration. Blue highlighted area signifies optical stimulation. B) Quantitative comparison of moEPSC amplitudes in Air (cell n = 9, rat n = 5) and CIE rats (cell n = 13, rat n = 7). C) Representative moEPSC traces in the presence of TTX and 4AP from an Air (top traces) and CIE (bottom traces) rat. In this and all other representative traces individual inputs are shown by thin gray lines while the average response amplitude is illustrated by a thicker overlaid black line. D-F) Quantitative comparison of oEPSC (Air cell n = 27, rat n = 11; CIE cell n = 25, rat n = 8) (D), oIPSC areas (Air cell n = 27, rat n = 11; CIE cell n = 24, rat n = 8) (E) and E/I area ratios Air cell n = 26, rat n = 11; CIE cell n = 22, rat n = 8 (F). G) Optical latencies of oPSCs. H) Representative traces of oEPSCs (upward deflecting traces) and oIPSCs (downward deflecting traces) obtained from Air (left) and CIE (right) rats. *$p < 0.05$, **$p < 0.01$ and errors are reported as ±SEM. (For interpretation of the references to colour in this figure legend, the reader is referred to the Web version of this article.)

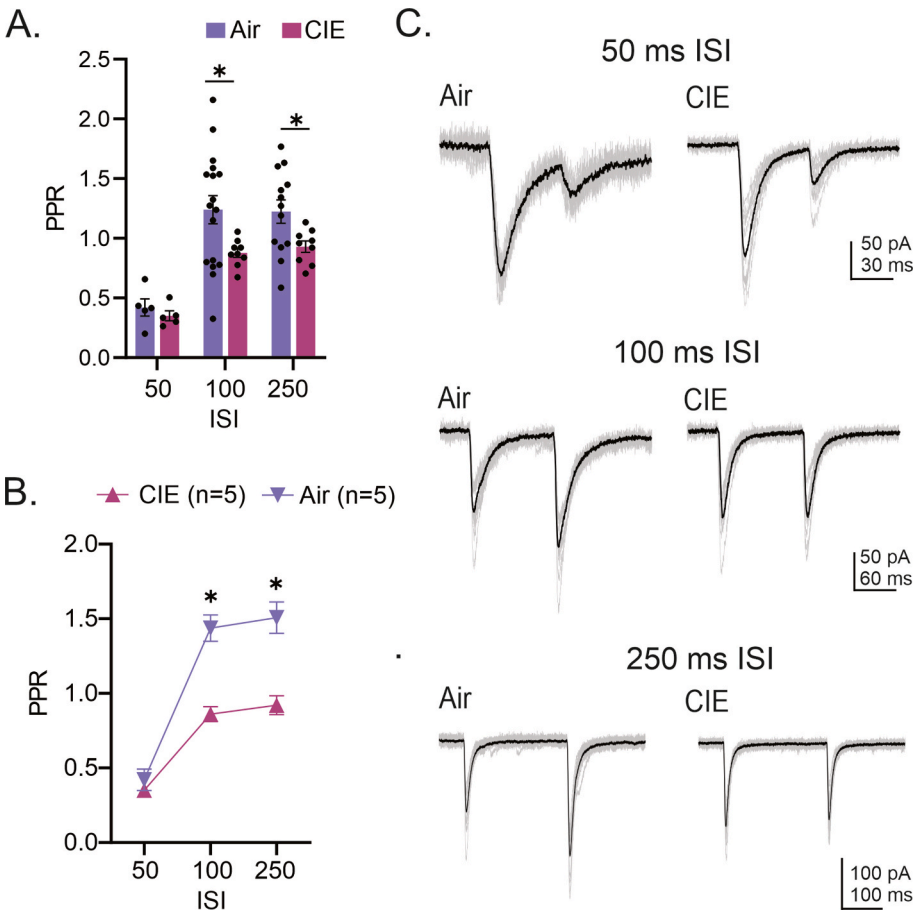

Fig. 2. Presynaptic release probability of BLA input onto vSub neurons is increased in CIE rats. A) Quantitative graphical comparison of all oPPrs at 50 (Air cell n = 5, rat n = 5; CIE cell n = 5, rat n = 4), 100 (Air cell n = 17, rat n = 10; CIE cell n = 9, rat n = 5) and 250 (Air cell n = 13, rat n = 9; CIE cell n = 9, rat n = 5) ms ISI between Air and CIE-treated rats B) Quantitative graphical comparison of all oPPrs at 50, 100 and 250 ms ISI between Air (cell n = 5, rat n = 5) and CIE-treated (cell n = 5, rat n = 4) rats in cells from which all three measures could be obtained in the same neuron. C) Representative traces of oEPSC PPrs at 50 (top traces), 100 (middle traces) and 250 (bottom traces) ms ISI. *p < 0.05 and errors are reported as ±SEM.

nature of these BLA-driven inputs we considered total charge transfer for the duration of the optically evoked BLA current in rACSF (in the absence of inhibitors) the most appropriate comparison to capture CIE-driven adaptations. We identified an increase in polysynaptic oEPSC (oEPSC) area of CIE-treated rats ($p = 0.0098$; Air cell n = 27, rat n = 11; CIE cell n = 25, rat n = 8; Mann-Whitney Test; Fig. 1D and G). Activation of BLA inputs also elicited inhibitory currents (oIPSC) to vSub neurons. For consistency with moEPSC measures we also compared oPSC amplitudes between Air and CIE rats. Using this measure we found a trend in oEPSC amplitude ($p = 0.057$, Mann-Whitney Test, data not graphically illustrated) and a significant effect on oIPSC amplitude ($p = 0.006$, Mann-Whitney Test, data not graphically illustrated).

In response to CIE we saw an increase in the area of these oIPSCs ($p = 0.0269$; Air cell n = 27, rat n = 11; CIE cell n = 24, rat n = 8; Mann-Whitney Test; Fig. 1E and G). By recording both excitatory and inhibitory inputs in the same neuron from a subset of cells we were able to compare the excitatory to inhibitory balance (E-I ratio) in response to CIE. CIE animals did not show a shift in their E-I ratio ($p = 0.665$; Air cell n = 26, rat n = 11; CIE cell n = 22, rat n = 8; Mann-Whitney Test; Fig. 1F and H).

In addition to these measures, we also assessed possible presynaptic adaptations using optically driven paired-pulse ratios (oPPrs) in the pBLA-vSub pathway. We measured PPrs of oEPSCs with interstimulus intervals (ISI) of 50, 100 and 250 ms. When including all PPR measures using a mixed-effect model, we identified no main effect of CIE ($F_{(1,25)} = 1.632$, $p = 0.2132$; Fig. 2A and C) with a significant effect of ISI ($F_{(1.673,22.59)} = 48.91$, $p < 0.0001$; Fig. 2A and C) and an interaction effect ($F_{(2,27)} = 4.785$, $p = 0.0166$; Fig. 2A and C). A multiple comparison post hoc analysis revealed a decrease in the PPR of CIE rats at an ISI of 100 ms ($p = 0.0033$; Air cell n = 17, rat n = 10; CIE cell n = 9, rat n = 5) and 250 ms ($p = 0.007$; Air cell n = 13, rat n = 9; CIE cell n = 9, rat n = 5), but not at 50 ms ($p > 0.9999$; Air cell n = 5, rat n = 5; CIE cell n = 5, rat n = 4; Fig. 2A and C). Additionally, we conducted a separate analysis in the subset of neurons (Air cell n = 5, rat n = 5; CIE cell n = 5, rat n = 4; Fig. 2B and C) for which all measures at all 3 ISIs were obtained. This analysis yielded very similar results with a main effect of ISI ($F_{(1.426,11.41)} = 89.51$, $p < 0.0001$; Fig. 2B and C) in addition to an effect of CIE ($F_{(1,8)} = 37.58$; $p = 0.0003$; Fig. 2B and C) and an interaction ($F_{(2,16)} = 9.212$, $p < 0.0022$; Fig. 2B and C). A post hoc analysis identified a decrease in the PPR of CIE rats at ISIs of 100 ms ($p = 0.0033$) and 250 ms ($p = 0.007$), but not at 50 ms ($p > 0.9999$) suggestive of a CIE-dependent increase in the release probability of pBLA-vSub inputs.

The difference in CIE-associated adaptations between mono- and polysynaptic pBLA-vSub inputs may have been driven, at least in part, by changes in intrinsic vSub network activity. To address this possibility, we recorded both spontaneous EPSCs and IPSCs (sEPSCs and sIPSCs, respectively) from vSub pyramidal neurons of AIR and CIE-treated animals. We found no change in sEPSC frequency ($p = 0.0753$; Air cell n = 18, rat n = 8, CIE n = 19, rat n = 7; Mann-Whitney Test; Fig. 3A and B), but did observe a significant increase in sIPSC frequency ($p = 0.0047$; Air n = 17; rat n = 7, CIE n = 18 rat n = 6; unpaired *t*-test; Fig. 3C and D). In contrast, CIE had no effect on the amplitude of either sEPSCs ($p = 0.0584$; Air n = 18, rat n = 8, CIE n = 19, rat n = 7; Mann-Whitney Test; Fig. 3A and B) or sIPSCs ($p = 0.0717$; Air n = 17, rat n = 7; CIE n = 18,

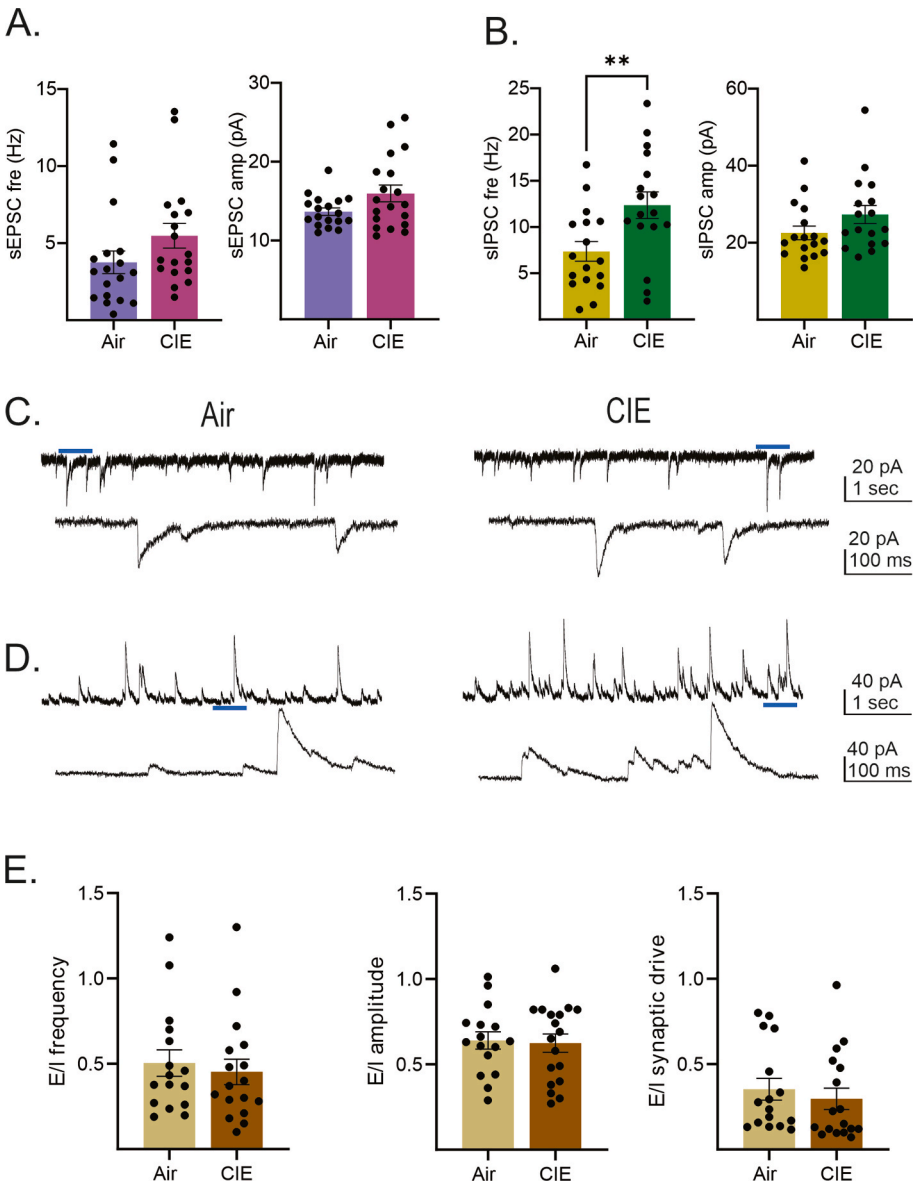

Fig. 3. Spontaneous inhibitory, but not excitatory, activity (sPSCs) is increased in CIE-treated rats. A) There is no CIE-dependent effect on sEPSC (Air n = 19, rat n = 8; CIE n = 19, rat n = 7) frequency (left graph) or amplitude (right graph). B) CIE elicits an increase in sIPSC (Air n = 17, rat n = 7; CIE n = 18, rat n = 6) frequency (left graph) but not amplitude (right graph). C) Representative sEPSC traces recorded from vSub neurons of Air (top two traces) and CIE (lower two traces) rats. D) Representative sIPSC traces recorded from vSub neurons of Air (top two traces) and CIE (lower two traces) rats. Blue line above upper traces indicate zoomed in section illustrated in lower traces. E) E/I ratios of sPSC frequency (left graph), amplitude (center graph) and synaptic drive (right graph) of Air and CIE-treated (Air cell n = 17; rat n = 8 CIE, cell n = 18, rat n = 6) rats. **$p < 0.01$ and errors are reported as ±SEM. (For interpretation of the references to colour in this figure legend, the reader is referred to the Web version of this article.)

rat n = 6; Mann-Whitney Test; Fig. 3C and D). We next sought to determine whether the E/I balance was affected by CIE. We found no effect on the E/I frequency ($p = 0.6598$; Mann-Whitney Test; Fig. 3E), amplitude ($p > 0.9999$; Mann-Whitney Test; Fig. 3F) or synaptic drive ($p = 0.2157$; Mann-Whitney Test, Fig. 3G) between Air and CIE rats (Air cell n = 17; rat n = 8 CIE, cell n = 18, rat n = 6). These findings indicate that, in female rats, CIE primarily increased the presynaptic release probability of inhibitory inputs without impacting postsynaptic spontaneous neurotransmission properties or the E/I balance of spontaneous activity.

The CIE-mediated increase in both BLA-driven GABAergic inputs and intrinsic vSub GABAergic transmission raised our interest in exploring whether blocking $GABA_A$ receptor-mediated inhibition would impact optically driven and spontaneous activity in the vSub. To explore this question, we conducted electrophysiological recordings in the presence of the $GABA_A$ receptor antagonist picrotoxin (PTX). To focus our investigation on AMPA receptor-mediated adaptations, we conducted our electrophysiological recordings at −80 mV (where non-GluN3 containing NMDA receptors remain under voltage-dependent block (Mayer et al., 1984) in the presence of PTX, while optically stimulating inputs arising from the BLA. Under these conditions we saw a robust increase in presumptive AMPA receptor-mediated excitatory polysynaptic vSub input in CIE rats ($p = 0.0087$; Air cell n = 19, rat n = 9; CIE cell n = 13, rat n = 7); Mann-Whitney Test; Fig. 4A and B). Additionally, we explored the effect of PTX on spontaneous activity by recording sEPSCs in the presence of PTX at −80 mV in vSub neurons. In the presence of PTX, CIE led to a robust increase in the frequency ($p = 0.0009$; Air cell n = 19, rat n = 8; CIE cell n = 13, rat n = 6; Mann-Whitney Test; Fig. 4C and D) of sEPSCs without a change in sEPSC amplitude ($p > 0.9999$; Mann-Whitney Test; Fig. 4C and D) indicative of

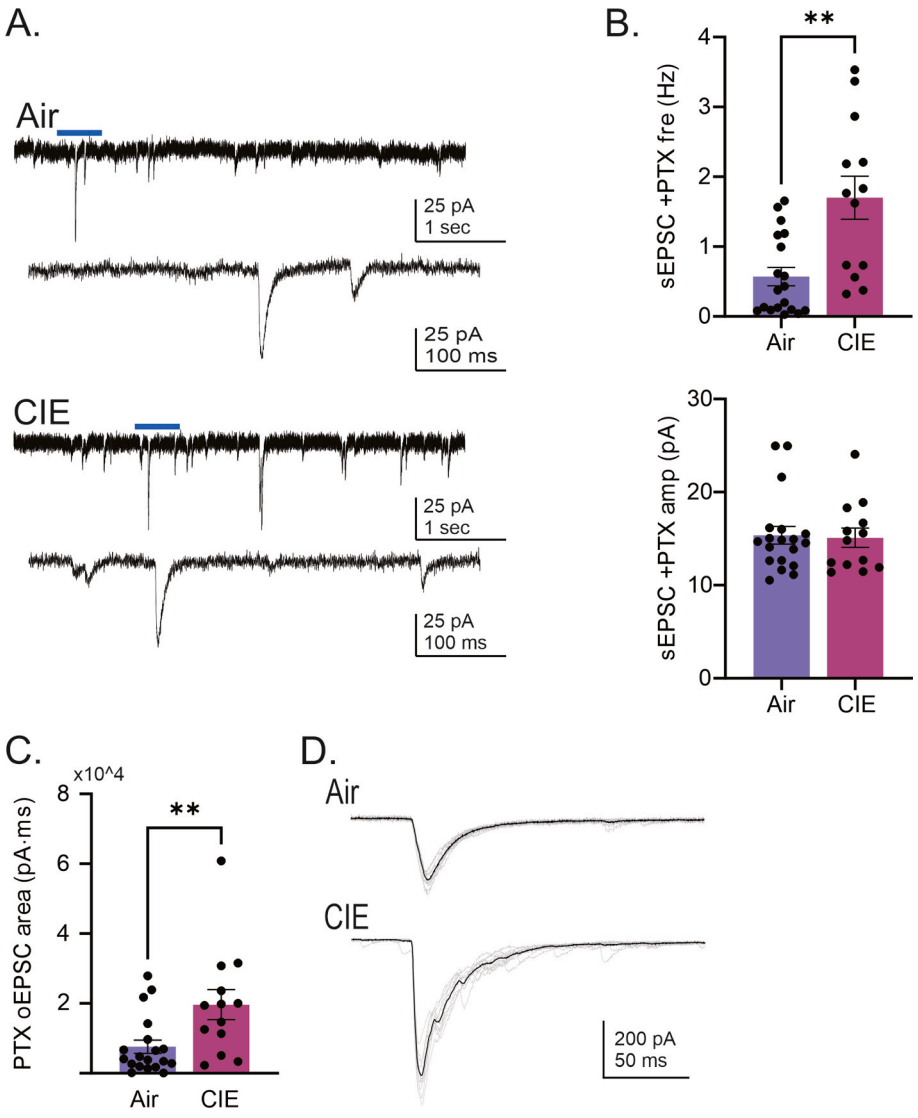

Fig. 4. Blocking $GABA_A$ -mediated inhibition in the vSub shows a robust strengthening of BLA-driven inputs and spontaneous activity of vSub neurons from CIE-treated rats. A) Quantitative comparison of disinhibited (presence of PTX) BLA-driven inputs in Air (cell n = 19, rat n = 9) and CIE-treated (cell n = 13, rat n = 7) rats. B) Representative recordings of oEPSCs at −80 mV in the presence of PTX. C) Representative recordings of sEPSCs at −80 mV in the presence of PTX from an Air (top) and CIE (bottom) rat. Blue line above upper traces indicate zoomed in section illustrated in lower traces. B) Quantitative comparison of disinhibited (presence of PTX) sEPSC frequency (top) and amplitude (bottom) in Air (cell n = 19, rat n = 8) and CIE-treated (cell n = 13, rat n = 6) rats. **p < 0.01, **p < 0.01, ***p < 0.001 and errors are reported as ±SEM. (For interpretation of the references to colour in this figure legend, the reader is referred to the Web version of this article.)

a presynaptic change in release probability that is unmasked by $GABA_A$ receptor-mediated disinhibition.

Finally, to further assess AMPA receptor-mediated inputs we conducted recordings of BLA-vSub oEPSCs while voltage clamping vSub neurons at positive potentials (+40 mV) in the presence of PTX to unmask NMDA receptor-mediated inputs. With our prior data indicating a lack of effect of CIE on monosynaptic BLA-vSub excitatory neurotransmission, our principal analysis was not limited to putative monosynaptic vSub oEPSCs. Subsequent to recording a baseline mixed AMPA/NMDA-receptor component we isolated the AMPA receptor-mediated current by applying the NMDA receptor antagonist, AP-5. This allowed us to determine the magnitude of the current contributed by each receptor and consequently the AMPA/NMDA ratio. This approach revealed a significant CIE-dependent increase in the AMPA/NMDA ratio ($p = 0.0047$; Air n = 8, cell n = 8; CIE cell n = 6, rat n = 6); unpaired *t*-test; Fig. 5A top graph and 5B). When possible, we adjusted stimulation parameters to capture putative monosynaptic BLA inputs. This analysis of moEPSCs also revealed an increase in the AMPA/NMDA ratio ($p = 0.029$; Air n = 6, CIE n = 4; unpaired *t*-test; Fig. 5A bottom graph and 5B).

4. Discussion

Increased synaptic excitation in the basolateral amygdala (BLA) and ventral hippocampus (vHC), as well as within a monosynaptic BLA-vHC circuit, are known to promote anxiety-like behaviors in male rodents (Bach et al., 2023; Chang and Gean, 2019; Chang et al., 2015; Felix-Ortiz et al., 2013; Pi et al., 2020; Rau et al., 2015). Prior work by us and others also suggests that a strengthening of this circuitry may contribute to anxiogenic behaviors that develop during withdrawal from chronic alcohol vapor exposure (CIE) (Bach et al., 2021b; Han et al., 2017; Morales et al., 2018; Price and McCool, 2022). We previously found that a 10 day CIE treatment followed by 24 h withdrawal increased anxiety-like behaviors in male and female rats, although these effects were more pronounced in males. Surprisingly, while extracellular vHC recordings taken at this same withdrawal timepoint revealed increased

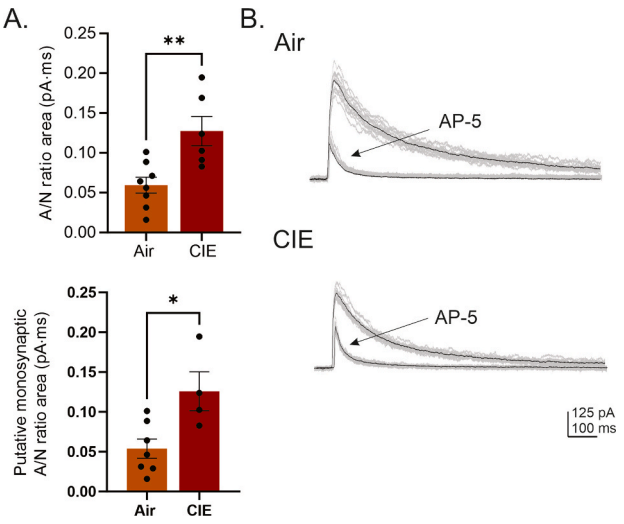

Fig. 5. AMPA/NMDA ratios are increased in vSub neurons of CIE rats. A) Quantitative comparison between Air and CIE rats show a strengthening of all putative mono- (lower graph; (Air n = 6, cell n = 6; CIE cell n = 4, rat n = 4) and combined mono- and poly (upper graph; Air n = 8, cell n = 8; CIE cell n = 6, rat n = 6) driven BLA AMPA/NMDA ratios of vSub neurons in response to CIE. B) Representative recordings of oEPSCs at +40 mV in the presence of PTX before and after the application of the NMDA receptor antagonist AP-5. **p < 0.01 and errors are reported as ±SEM.

excitability in recordings from males, a decrease in vHC synaptic excitation was observed in females (Bach et al., 2021a; Ewin et al., 2019; Pi et al., 2020). We recently followed up on these observations in males and also investigated the effects of CIE on the BLA projection to the vHC that is known to play a role in anxiety-like behaviors. As noted earlier, we discovered that vHC projecting BLA neurons innervate the ventral subiculum (vSub) and found that CIE led to increases in postsynaptic measures of synaptic excitability in the BLA-vSub circuit (e.g. AMPA/NMDA ratio, E/I ratio) as well as a presynaptic increase in spontaneous excitatory, but not inhibitory, intrinsic vSub synaptic transmission (Bach et al., 2021). The present experiments, conducted in females, were designed to replicate the methodology of this prior study examining the effects of CIE on BLA-vSub transmission and intrinsic vSub synaptic activity to gain mechanistic insight into the sexually dimorphic effects of CIE that we had previously observed.

Our findings revealed that the BLA also strongly innervates the vSub of female rats. However, CIE had no effect on postsynaptic monosynaptically-driven excitatory neurotransmission but did increase the release probability (decrease in PPR) in the BLA-vSub pathway in females in contrast to our prior findings in male rats where post- but not presynaptic monosynaptically driven excitatory BLA inputs were increased in CIE rats. When looking more broadly at BLA-vSub inputs composed of both mono- and polysynaptically-driven inputs, female rats did show an increase in both excitatory and inhibitory neurotransmission, similar to what we observed in males. However, unlike males, these adaptations were not associated with significant changes in E-I balance. We also discovered that CIE had sexually dimorphic effects on spontaneous vSub synaptic transmission, in that it led to a robust increase in sIPSC frequency in females, a finding we did not observe in males. Importantly, blocking $GABA_A$ receptors unmasked a significant CIE-associated increase in both BLA-vSub excitability and sEPSC frequency in female rats.

Overall, these findings suggest that intrinsic synaptic activity in the vSub is a principal driver of CIE-mediated adaptations, and that this treatment has sexually dimorphic effects on vSub synaptic plasticity. While spontaneous inhibitory, but not excitatory, activity was increased in female rats, the opposite was true in males. Since inhibition of GABAergic transmission elicited a CIE-mediated increase in sEPSC frequency in both sexes, these data suggest that the increase in intrinsic inhibition in females prevented the CIE-associated intrinsic hyperexcitability observed in males. Notably, we also found that putative monosynaptic AMPAR-mediated postsynaptic conductance (Fig. 1) was not increased in CIE-treated females unless $GABA_A$-R mediated inhibition was blocked which led to an increase in both overall optical input (mono- and polysynaptic) as well as putative monosynaptic AMPA-NMDA ratios. The combination of these findings suggests that, in females, $GABA_A$-R mediated inhibition provides an inhibitory shunt on both intrinsic glutamatergic transmission (sEPSC events) as well as BLA-driven postsynaptic excitatory inputs (mono-as well as overall optical input) sufficient to block CIE-associated hyperexcitability in this circuit. For monosynaptic BLA inputs, a likely explanation is that CIE strengthens a recently discovered monosynaptic GABAergic projection from the BLA to vHC (vCA1 and vSub) that plays a prominent role in modulating projection-specific behavior (AlSubaie et al., 2021). Our preliminary data indicates that this projection is sufficient to elicit a significant reduction in the strength of monosynaptic glutamatergic input, further arguing that this GABAergic conductance can directly impact monosynaptic BLA-vSub excitatory input. Future studies are underway to explore the role of this novel BLA-vSub GABAergic projection in our CIE model.

Our PPR results indicating an increase in release probability in the absence of $GABA_A$-R mediated inhibition are intriguing for two reasons. The first is that this presumptive increase in release probability was only seen at more prolonged ISIs. PPR release probability assessments are most commonly made at ISIs of 50 ms or less for glutamatergic synapses as even modulatory effects of many metabotropic presynaptic receptors can typically be captured at ISIs of 50 ms or less. Our failure to detect PPR changes at ISIs of 50 ms, with a reduction at both 100 and 250 ms, may thus point at the presynaptic mechanism driving this adaptation, assuming electrical and optical stimulation have similar temporal dynamics (Jackman et al., 2014; Maroto et al., 2023; Pouille and Schoppa, 2018). Receptors that have been implicated at other synapses to modulate release probability at more prolonged ISIs include $GABA_B$ as well as endocannabinoid receptors (Maroto et al., 2023; Salio et al., 2017). Future studies will aim to identify the underlying mechanism of this CIE-associated presynaptic adaptation. The second surprising aspect of our PPR findings is that this putative presynaptic adaptation was observed in the absence of a change in sEPSC frequency, which also typically reflects presynaptic function. This discrepancy is likely explained by the fact that only 10% of inputs to vSub neurons arises from non-hippocampal regions, including the BLA, although when activated this input has a robust modulatory effect on anxiety-like behavior (Felix-Ortiz et al., 2013; Pi et al., 2020; Wee and MacAskill, 2020). The PPR effect is therefore likely masked by non-BLA driven inputs onto vSub neurons, but the BLA-driven inputs may contribute to the trending increase of sEPSC frequencies we observed.

The sex-dependent inhibitory adaptations are both intriguing as well as somewhat counterintuitive juxtaposed to adaptations of neuronal activity typically seen in preclinical models of anxiety, AUD and the available evidence in clinical studies (Bach et al., 2021a; Blume et al., 2019; Hernandez-Avila et al., 2004; Lack et al., 2007; Randall et al., 1999; Rau et al., 2015; Towers et al., 2023). In preclinical anxiety models, increases in BLA and vHC activity as well as BLA-vHC excitation has been associated with heightened levels of anxiety-like behavior (Bach et al., 2023; Felix-Ortiz et al., 2013; Rau et al., 2015; Silberman et al., 2009). Moreover, the frequent comorbidity that exists between anxiety disorders and AUD would lead one to predict that CIE increases excitability in these brain regions and circuit; a relationship we found to hold true in our prior studies in male rats (Bach et al., 2021a; Ewin et al., 2019). Prior behavioral evidence with CIE-treated female rats has shown more mixed findings, suggesting that female rats exposed to a 'traditional' 10-day CIE paradigm may be less susceptible to developing anxiety-like behaviors (Bach et al., 2021b; Ewin et al., 2019; Lack et al., 2007; Morales et al., 2018). One caveat that remains is that behavioral

studies looking at anxiety-like behavior mediated by the BLA to vHC projection have been limited to male subjects, leaving open the possibility that the circuit does not modulate these behaviors in female rats or does so in a functionally distinct manner. Nonetheless our current functional data indicating that CIE enhances BLA-vSub inhibition as well as excitation along with intrinsic vSub GABAergic inhibition, supports the idea that female rats may be less susceptible to CIE and that sexually dimorphic adaptations in vSub inhibition may play an important mechanistic role in explaining these behavioral findings. Given that CIE is generally considered a model of alcohol dependence, this finding seems counterintuitive relative to most epidemiological data. In clinical populations, AUD remains more common in men, but heavy drinking women often experience more profound negative consequences and a heightened propensity to transition to AUD and associated comorbid conditions (Guinle and Sinha, 2020; Hernandez-Avila et al., 2004; Towers et al., 2023).

As in many such comparative analyses between clinical and preclinical studies, direct comparisons are plagued by a plethora of confounding factors. One such factor is that preclinical AUD models generally introduce alcohol to experimental subjects during adulthood. In humans, alcohol use is commonly initiated during adolescence or early adulthood and early onset alcohol exposure is strongly linked with increased risk of AUD (Jones et al., 2018). Adolescence and early adulthood are also periods of rapid hormone level changes that can profoundly influence synaptic plasticity (see additional discussion below). Indeed, there is emerging evidence from rodent and clinical studies that adolescence may be a particularly vulnerable period to experience excessive (or even moderate) alcohol exposure (Chassin et al., 2002; Creswell et al., 2020; Guinle and Sinha, 2020; McCool and McGinnis, 2020; Sicher et al., 2023). Thus, it will be important to consider how the sex differences in CIE-dependent synaptic adaptations that we have observed are influenced by CIE exposure during adolescence. Another important factor may be the duration of alcohol exposure used in preclinical CIE models. The normal progression of AUD typically involves the gradual development of pathologic levels of alcohol consumption over the course of months or years and the neural adaptations that develop in men and women during the first weeks of alcohol drinking are not known. These factors raise the question of whether the increase in vSub GABAergic inhibition that we observed in females following a relatively brief 10 day CIE treatment would persist with longer exposure durations. If this adaptation is transient, it is possible that longer more clinically-relevant CIE exposures could elicit similar maladaptive hyperexcitability in both sexes. Indeed, an early study found that a nine day chronic alcohol liquid diet significantly increased sensitivity to withdrawal-induced seizures triggered by the $GABA_A$ receptor antagonist bicuculline in male, but not female rats whereas after 14 days on the liquid diet, bicuculline withdrawal seizures thresholds were similar in both sexes (Devaud and Chadda, 2001). Moreover, a more recent study exploring CIE-dependent plasticity within the BLA of male and female rats found that females develop adaptations mimicking those of their male counterparts but at a slower progression. Notably, this study determined that presynaptic plasticity precedes postsynaptic adaptations (Morales et al., 2018). Our data identifying only pre-, but not postsynaptic, adaptations in the BLA-vSub pathway in female rats when we identified the opposite in male rats (post, but not presynaptic changes) would thus be congruent with the overall hypothesis that females may initially be protected from CIE-associated hyperexcitability through an elevation in GABAergic inhibition that may be overcome by more prolonged CIE exposures. Indeed, our preliminary data suggest that while a 10 day CIE treatment had no effect on anxiety measures in the elevated plus-maze, withdrawal from a longer 30 day exposure did significantly increase anxiety-like behavior on this assay.

Independent of our understanding of what these sex-dependent CIE adaptations mean, it is also important to consider the underlying mechanism(s) that give rise to them. Sex hormones are one likely suspect. Alcohol can directly impact steroid hormones and steroid hormones can in turn affect drinking behaviors (Erol et al., 2019; McCool and McGinnis, 2020). As already noted, these interactions make adolescence and puberty a particularly vulnerable period for alcohol consumption in both sexes that can facilitate neuronal adaptations lasting into adulthood and increasing an individual's vulnerability to develop AUD (Jones et al., 2018; Sicher et al., 2023). Our study only tested the impacts of CIE during adulthood in previously ethanol-naïve rats. Future studies are needed to address the effect of adolescent drinking and/or adolescent CIE exposure on BLA and vSub synaptic transmission. The hormonal flunctions associated with the menstrual/estrous cycle represents yet another factor that could drive neuronal adaptations that are specific to biologic females. In our study we did not track the estrous cycle of our rats. Previous studies have indicated that female rats undergoing a CIE paradigm experience a disrupted estrous cycle with the majority of females getting arrested in diestrus (Morales et al., 2018). Whether the estrous cycle impacts basal neuronal activity patterns in the BLA-vSub pathway or vSub, as has been shown in other brain regions, of our control subjects that may influence comparative measures of female rats undergoing a CIE paradigm will be the subject of future studies.

In summary, these studies on CIE-associated adaptations of the BLA-vSub circuit and intrinsic vSub connectivity in female rats revealed robust sex-dependent adaptations when compared to an earlier study in males. In male rats, a 24 h withdrawal following a 10 day CIE treatment led to significant hyperexcitability, while this same exposure regimen resulted in a facilitation of GABAergic inhibition in females that may have contributed to the maintenance of a normal E-I balance (BLA-vSub pathway) during withdrawal, likely mediated primarily by a CIE-associated strengthening of intrinsic vSub inhibition. This finding suggests that female rats may be resilient to the initial BLA-vSub and intrinsic vSub hyperexcitability promoted by withdrawal from a relatively short CIE regimen. Additional studies will be needed to determine if this resilient phenotype persists with longer CIE exposures and to resolve the mechanisms responsible for the sexually dimorphic synaptic effects of CIE that we have uncovered, particularly the impact of adolescent alcohol drinking and CIE on pubertal development and the estrous cycle. Collectively, our findings add to a rapidly increasing body of evidence demonstrating profound sex differences in the maladaptive synaptic alterations that arise following chronic alcohol exposure and a need for additional work to better understand the neurobiological processes underlying these differences and whether findings like these point toward the need for the development of sex-specific therapeutic approaches to combat AUD.

Funding

This work was supported by the National Institutes of Health [grant numbers: K01 AA030081 (ECB), P50 AA026117 (JLW), R37 AA017531 (JLW).

CRediT authorship contribution statement

Eva C. Bach: Writing – review & editing, Writing – original draft, Project administration, Methodology, Investigation, Funding acquisition, Formal analysis, Data curation, Conceptualization. **Jeff L. Weiner:** Writing – review & editing, Supervision, Project administration, Funding acquisition, Conceptualization.

Declaration of competing interest

The authors declare that they have no competing financial interests or personal relationships that could have appeared to influence the work reported in this paper.

References

Almonte, A.G., Ewin, S.E., Mauterer, M.I., Morgan, J.W., Carter, E.S., Weiner, J.L., 2017. Enhanced ventral hippocampal synaptic transmission and impaired synaptic plasticity in a rodent model of alcohol addiction vulnerability. Sci. Rep. 7 (1), 12300. https://doi.org/10.1038/s41598-017-12531-z.

AlSubaie, R., Wee, R.W., Ritoux, A., Mishchanchuk, K., Passlack, J., Regester, D., MacAskill, A.F., 2021. Control of parallel hippocampal output pathways by amygdalar long-range inhibition. Elife 10. https://doi.org/10.7554/eLife.74758.

Bach, E.C., Ewin, S.E., Baldassaro, A.D., Carlson, H.N., Weiner, J.L., 2021a. Chronic intermittent ethanol promotes ventral subiculum hyperexcitability via increases in extrinsic basolateral amygdala input and local network activity. Sci. Rep. 11 (1), 8749. https://doi.org/10.1038/s41598-021-87899-0.

Bach, E.C., Ewin, S.E., Heaney, C.F., Carlson, H.N., Ortelli, O.A., Almonte, A.G., Weiner, J.L., 2023. Chemogenetic inhibition of a monosynaptic projection from the basolateral amygdala to the ventral hippocampus selectively reduces appetitive, but not consummatory, alcohol drinking-related behaviours. Eur. J. Neurosci. 57 (8), 1241–1259. https://doi.org/10.1111/ejn.15944.

Bach, E.C., Morgan, J.W., Ewin, S.E., Barth, S.H., Raab-Graham, K.F., Weiner, J.L., 2021b. Chronic ethanol exposures leads to a negative affective state in female rats that is accompanied by a paradoxical decrease in ventral Hippocampus excitability. Front. Neurosci. 15, 669075. https://doi.org/10.3389/fnins.2021.669075.

Bannerman, D.M., Rawlins, J.N., McHugh, S.B., Deacon, R.M., Yee, B.K., Bast, T., Feldon, J., 2004. Regional dissociations within the hippocampus–memory and anxiety. Neurosci. Biobehav. Rev. 28 (3), 273–283. https://doi.org/10.1016/j.neubiorev.2004.03.004.

Blaine, S.K., Sinha, R., 2017. Alcohol, stress, and glucocorticoids: from risk to dependence and relapse in alcohol use disorders. Neuropharmacology 122, 136–147. https://doi.org/10.1016/j.neuropharm.2017.01.037.

Blume, S.R., Freedberg, M., Vantrease, J.E., Chan, R., Padival, M., Record, M.J., Rosenkranz, J.A., 2017. Sex- and estrus-dependent differences in rat basolateral amygdala. J. Neurosci. 37 (44), 10567–10586. https://doi.org/10.1523/JNEUROSCI.0758-17.2017.

Blume, S.R., Padival, M., Urban, J.H., Rosenkranz, J.A., 2019. Disruptive effects of repeated stress on basolateral amygdala neurons and fear behavior across the estrous cycle in rats. Sci. Rep. 9 (1), 12292. https://doi.org/10.1038/s41598-019-48683-3.

Chang, C.H., Gean, P.W., 2019. The ventral Hippocampus controls stress-provoked impulsive aggression through the ventromedial hypothalamus in post-weaning social isolation mice. Cell Rep. 28 (5), 1195–1205. https://doi.org/10.1016/j.celrep.2019.07.005 e1193.

Chang, C.H., Hsiao, Y.H., Chen, Y.W., Yu, Y.J., Gean, P.W., 2015. Social isolation-induced increase in NMDA receptors in the hippocampus exacerbates emotional dysregulation in mice. Hippocampus 25 (4), 474–485. https://doi.org/10.1002/hipo.22384.

Chappell, A.M., Carter, E., McCool, B.A., Weiner, J.L., 2013. Adolescent rearing conditions influence the relationship between initial anxiety-like behavior and ethanol drinking in male Long Evans rats. Alcohol Clin. Exp. Res. 37 (Suppl. 1), E394–E403. https://doi.org/10.1111/j.1530-0277.2012.01926.x. Suppl 1.

Chassin, L., Pitts, S.C., Prost, J., 2002. Binge drinking trajectories from adolescence to emerging adulthood in a high-risk sample: predictors and substance abuse outcomes. J. Consult. Clin. Psychol. 70 (1), 67–78. Retrieved from. https://www.ncbi.nlm.nih.gov/pubmed/11860058.

Christian, D.T., Alexander, N.J., Diaz, M.R., Robinson, S., McCool, B.A., 2012. Chronic intermittent ethanol and withdrawal differentially modulate basolateral amygdala AMPA-type glutamate receptor function and trafficking. Neuropharmacology 62 (7), 2430–2439. https://doi.org/10.1016/j.neuropharm.2012.02.017.

Creswell, K.G., Chung, T., Skrzynski, C.J., Bachrach, R.L., Jackson, K.M., Clark, D.B., Martin, C.S., 2020. Drinking beyond the binge threshold in a clinical sample of adolescents. Addiction 115 (8), 1472–1481. https://doi.org/10.1111/add.14979.

Devaud, L.L., Chadda, R., 2001. Sex differences in rats in the development of and recovery from ethanol dependence assessed by changes in seizure susceptibility. Alcohol Clin. Exp. Res. 25 (11), 1689–1696. Retrieved from. https://www.ncbi.nlm.nih.gov/pubmed/11707644.

Erol, A., Ho, A.M., Winham, S.J., Karpyak, V.M., 2019. Sex hormones in alcohol consumption: a systematic review of evidence. Addiction Biol. 24 (2), 157–169. https://doi.org/10.1111/adb.12589.

Ewin, S.E., Morgan, J.W., Niere, F., McMullen, N.P., Barth, S.H., Almonte, A.G., Weiner, J.L., 2019. Chronic intermittent ethanol exposure selectively increases synaptic excitability in the ventral domain of the rat Hippocampus. Neuroscience 398, 144–157. https://doi.org/10.1016/j.neuroscience.2018.11.028.

Felix-Ortiz, A.C., Beyeler, A., Seo, C., Leppla, C.A., Wildes, C.P., Tye, K.M., 2013. BLA to vHPC inputs modulate anxiety-related behaviors. Neuron 79 (4), 658–664. https://doi.org/10.1016/j.neuron.2013.06.016.

Felix-Ortiz, A.C., Burgos-Robles, A., Bhagat, N.D., Leppla, C.A., Tye, K.M., 2016. Bidirectional modulation of anxiety-related and social behaviors by amygdala projections to the medial prefrontal cortex. Neuroscience 321, 197–209. https://doi.org/10.1016/j.neuroscience.2015.07.041.

Flores-Bonilla, A., Richardson, H.N., 2020. Sex differences in the neurobiology of alcohol use disorder. Alcohol Res 40 (2), 4. https://doi.org/10.35946/arcr.v40.2.04.

Giacometti, L.L., Barker, J.M., 2020. Sex differences in the glutamate system: implications for addiction. Neurosci. Biobehav. Rev. 113, 157–168. https://doi.org/10.1016/j.neubiorev.2020.03.010.

Gilpin, N.W., Weiner, J.L., 2017. Neurobiology of comorbid post-traumatic stress disorder and alcohol-use disorder. Gene Brain Behav. 16 (1), 15–43. https://doi.org/10.1111/gbb.12349.

Grace, S., Rossetti, M.G., Allen, N., Batalla, A., Bellani, M., Brambilla, P., Lorenzetti, V., 2021. Sex differences in the neuroanatomy of alcohol dependence: hippocampus and amygdala subregions in a sample of 966 people from the ENIGMA Addiction Working Group. Transl. Psychiatry 11 (1), 156. https://doi.org/10.1038/s41398-021-01204-1.

Grant, B.F., Chou, S.P., Saha, T.D., Pickering, R.P., Kerridge, B.T., Ruan, W.J., Hasin, D. S., 2017. Prevalence of 12-month alcohol use, high-risk drinking, and DSM-IV alcohol use disorder in the United States, 2001-2002 to 2012-2013: results from the national epidemiologic survey on alcohol and related conditions. JAMA Psychiatr. 74 (9), 911–923. https://doi.org/10.1001/jamapsychiatry.2017.2161.

Guinle, M.I.B., Sinha, R., 2020. The role of stress, trauma, and negative affect in alcohol misuse and alcohol use disorder in women. Alcohol Res 40 (2), 5. https://doi.org/10.35946/arcr.v40.2.05.

Han, B.H., Moore, A.A., Sherman, S., Keyes, K.M., Palamar, J.J., 2017. Demographic trends of binge alcohol use and alcohol use disorders among older adults in the United States, 2005-2014. Drug Alcohol Depend. 170, 198–207. https://doi.org/10.1016/j.drugalcdep.2016.11.003.

Hernandez-Avila, C.A., Rounsaville, B.J., Kranzler, H.R., 2004. Opioid-, cannabis- and alcohol-dependent women show more rapid progression to substance abuse treatment. Drug Alcohol Depend. 74 (3), 265–272. https://doi.org/10.1016/j.drugalcdep.2004.02.001.

Jackman, S.L., Beneduce, B.M., Drew, I.R., Regehr, W.G., 2014. Achieving high-frequency optical control of synaptic transmission. J. Neurosci. 34 (22), 7704–7714. https://doi.org/10.1523/JNEUROSCI.4694-13.2014.

Jones, S.A., Lueras, J.M., Nagel, B.J., 2018. Effects of binge drinking on the developing brain. Alcohol Res 39 (1), 87–96. Retrieved from. https://www.ncbi.nlm.nih.gov/pubmed/30557151.

Kim, S.Y., Adhikari, A., Lee, S.Y., Marshel, J.H., Kim, C.K., Mallory, C.S., Deisseroth, K., 2013. Diverging neural pathways assemble a behavioural state from separable features in anxiety. Nature 496 (7444), 219–223. https://doi.org/10.1038/nature12018.

Kondev, V., Najeed, M., Yasmin, F., Morgan, A., Loomba, N., Johnson, K., Patel, S., 2023. Endocannabinoid release at ventral hippocampal-amygdala synapses regulates stress-induced behavioral adaptation. Cell Rep. 42 (9), 113027. https://doi.org/10.1016/j.celrep.2023.113027.

Koob, G.F., Volkow, N.D., 2016. Neurobiology of addiction: a neurocircuitry analysis. Lancet Psychiatr. 3 (8), 760–773. https://doi.org/10.1016/S2215-0366(16)00104-8.

Lack, A.K., Diaz, M.R., Chappell, A., DuBois, D.W., McCool, B.A., 2007. Chronic ethanol and withdrawal differentially modulate pre- and postsynaptic function at glutamatergic synapses in rat basolateral amygdala. J. Neurophysiol. 98 (6), 3185–3196. https://doi.org/10.1152/jn.00189.2007.

Levine, O.B., Skelly, M.J., Miller, J.D., Rivera-Irizarry, J.K., Rowson, S.A., DiBerto, J.F., Pleil, K.E., 2021. The paraventricular thalamus provides a polysynaptic brake on limbic CRF neurons to sex-dependently blunt binge alcohol drinking and avoidance behavior in mice. Nat. Commun. 12 (1), 5080. https://doi.org/10.1038/s41467-021-25368-y.

Maroto, I.B., Costas-Insua, C., Berthoux, C., Moreno, E., Ruiz-Calvo, A., Montero-Fernandez, C., Guzman, M., 2023. Control of a hippocampal recurrent excitatory circuit by cannabinoid receptor-interacting protein Gap43. Nat. Commun. 14 (1), 2303. https://doi.org/10.1038/s41467-023-38026-2.

Mayer, M.L., Westbrook, G.L., Guthrie, P.B., 1984. Voltage-dependent block by Mg2+ of NMDA responses in spinal cord neurones. Nature 309 (5965), 261–263. https://doi.org/10.1038/309261a0.

McCool, B.A., McGinnis, M.M., 2020. Adolescent vulnerability to alcohol use disorder: neurophysiological mechanisms from preclinical studies. Handb. Exp. Pharmacol. 258, 421–442. https://doi.org/10.1007/164_2019_296.

Morales, M., McGinnis, M.M., Robinson, S.L., Chappell, A.M., McCool, B.A., 2018. Chronic intermittent ethanol exposure modulation of glutamatergic neurotransmission in rat lateral/basolateral amygdala is duration-, input-, and sex-dependent. Neuroscience 371, 277–287. https://doi.org/10.1016/j.neuroscience.2017.12.005.

Pi, G., Gao, D., Wu, D., Wang, Y., Lei, H., Zeng, W., Wang, J.Z., 2020. Posterior basolateral amygdala to ventral hippocampal CA1 drives approach behaviour to exert an anxiolytic effect. Nat. Commun. 11 (1), 183. https://doi.org/10.1038/s41467-019-13919-3.

Pouille, F., Schoppa, N.E., 2018. Cannabinoid receptors modulate excitation of an olfactory bulb local circuit by cortical feedback. Front Cell Neurosci. 12, 47. https://doi.org/10.3389/fncel.2018.00047.

Price, M.E., McCool, B.A., 2022. Chronic alcohol dysregulates glutamatergic function in the basolateral amygdala in a projection-and sex-specific manner. Front. Cell. Neurosci. 16, 857550. https://doi.org/10.3389/fncel.2022.857550.

Randall, C.L., Roberts, J.S., Del Boca, F.K., Carroll, K.M., Connors, G.J., Mattson, M.E., 1999. Telescoping of landmark events associated with drinking: a gender comparison. J. Stud. Alcohol 60 (2), 252–260. https://doi.org/10.15288/jsa.1999.60.252.

Rau, A.R., Chappell, A.M., Butler, T.R., Ariwodola, O.J., Weiner, J.L., 2015. Increased basolateral amygdala pyramidal cell excitability may contribute to the anxiogenic phenotype induced by chronic early-life stress. J. Neurosci. 35 (26), 9730–9740. https://doi.org/10.1523/JNEUROSCI.0384-15.2015.

Salio, C., Merighi, A., Bardoni, R., 2017. GABA(B) receptors-mediated tonic inhibition of glutamate release from Abeta fibers in rat laminae III/IV of the spinal cord dorsal horn. Mol. Pain 13, 1744806917710041. https://doi.org/10.1177/1744806917710041.

Sicher, A.R., Starnes, W.D., Griffith, K.R., Dao, N.C., Smith, G.C., Brockway, D.F., Crowley, N.A., 2023. Adolescent binge drinking leads to long-lasting changes in

cortical microcircuits in mice. Neuropharmacology 234, 109561. https://doi.org/10.1016/j.neuropharm.2023.109561.

Silberman, Y., Bajo, M., Chappell, A.M., Christian, D.T., Cruz, M., Diaz, M.R., Weiner, J. L., 2009. Neurobiological mechanisms contributing to alcohol-stress-anxiety interactions. Alcohol 43 (7), 509–519. https://doi.org/10.1016/j.alcohol.2009.01.002.

Smith, A.J., Owens, S., Forsythe, I.D., 2000. Characterisation of inhibitory and excitatory postsynaptic currents of the rat medial superior olive. J. Physiol. 529 (Pt 3), 681–698. https://doi.org/10.1111/j.1469-7793.2000.00681.x. Pt 3.

Towers, E.B., Williams, I.L., Qillawala, E.I., Rissman, E.F., Lynch, W.J., 2023. Sex/Gender differences in the time-course for the development of substance use disorder: a focus on the telescoping effect. Pharmacol. Rev. 75 (2), 217–249. https://doi.org/10.1124/pharmrev.121.000361.

Vantrease, J.E., Avonts, B., Padival, M., DeJoseph, M.R., Urban, J.H., Rosenkranz, J.A., 2022. Sex differences in the activity of basolateral amygdalar neurons that project to the bed nucleus of the stria terminalis and their role in anticipatory anxiety. J. Neurosci. 42 (22), 4488–4504. https://doi.org/10.1523/JNEUROSCI.1499-21.2022.

Wee, R.W.S., MacAskill, A.F., 2020. Biased connectivity of brain-wide inputs to ventral subiculum output neurons. Cell Rep. 30 (11), 3644–3654. https://doi.org/10.1016/j.celrep.2020.02.093 e3646.

White, A., Castle, I.J., Chen, C.M., Shirley, M., Roach, D., Hingson, R., 2015. Converging patterns of alcohol use and related outcomes among females and males in the United States, 2002 to 2012. Alcohol Clin. Exp. Res. 39 (9), 1712–1726. https://doi.org/10.1111/acer.12815.